CHALMERS

Report

Wave farm collection grid analysis and design

Lluís Trilla and Torbjörn Thiringer

Division of Electric Power Engineering
Chalmers University of Technology
Gothenburg, Sweden 2013

Power Electronics and Electrical Engineering Area
Catalonia Institute for Energy Research (IREC)
Polytechnic University of Catalonia (UPC)
Barcelona, Spain 2013

Wave farm collection grid analysis and design

Technical report 2013:5

Department of Energy and Environtment

Division of Electric Power Engineering

CHALMERS UNIVERSITY OF TECHNOLOGY

SE-412 96 Göteborg

Sweden

Report

Members : IREC, Chalmers University and OHT
Date : 06 / 2013
Task : Wave farm collection grid analysis

Abstract

In this report, the collection grid of a wave farm is designed and analysed, the system under consideration goes from the connection point at each power converter (included in each wave energy unit) up to the point of common connection with the main grid. Time series that have been provided by Ocean Harvesting Technologies (OHT), being obtained from their simulation models for a scaled prototype and include data for mild, medium and strong sea states. The simulation models have been validated against small scale tank testing of a prime mover, a wave rider buoy, and scaled testing of the power take-off in a land based test-rig. Wave data is taken from EMEC, Scotland [7].

The design of the collection grid aims to optimize its size by minimizing its cost while maximizing the power output. For the economical assessment three layouts are taken into account and several scenarios for different energy prices and interest rates are presented. A life-cycle analysis is also done where the entire life span of the collection grid is considered showing that around 30€/MWh will be the share of the electricity price required to install and operate the collection grid.

The power quality of the resultant layout and its compliance with the grid code of the UK are analysed as well. This analysis includes power factor and voltage fluctuation estimation, line-fault ride-through assessment and flicker contribution analysis. Given the pulsating nature of the wave power systems special emphasis in the study of flicker emissions is done concluding that the proposed wave park is within the grid code limitations and even a reduction of a 66% in the flicker coefficients is reported when considering the aggregation of several units in one model.

1. Introduction

Ocean energy has the potential to play an important role as a renewable energy source. There are different forms of renewable energy available in the oceans such as waves or tides. The available wave power resource in the European area achieves about 290 GW and the world wide sea wave energy contribution is estimated to be about a 10% of the total energy consumption [4].

Most wave power technologies are at early stages, focusing on energy capture and conversion to electricity, these developments are resulting in a wide variety of strategies and designs. Many efforts are in commercial development and simplifying the mechanical complexity. In this sense Ocean Harvesting Technologies (OHT) provides a new design where the motion of a wave rider buoy is used to capture the energy contained in the incident wave and store this energy in a gravity weight accumulator in the form of potential energy. This accumulator acts as an energy buffer that is coupled to the generator smoothing the power output. Time series that have been provided by OHT, being obtained from their simulation models for a scaled prototype have been used throughout this report.

The energy captured by a single WEC presents high variations which cause large voltage fluctuations in the grid voltage. In order to reduce the power output fluctuation an important energy storage capacity is necessary. The potential for integration of wave power into the electrical system has to be studied since its degree of penetration will depend on the adverse impact it might have on the power network. In the development of WECs, grid integration is usually the last stage and therefore the least explored, as a consequence only few devices have been tested in grid-connected [5]. The analysis of the grid integration of the device may provide feedback that helps to improve the design of the WEC. To this end a layout for a collection grid and transmission to shore is proposed based on technical and economical aspects for a specific wave park configuration.

Because of the fluctuations generated by oscillating WECs a wave park may have a negative impact on the power quality of the local grid. The negative effects will come mainly from the excess in voltage fluctuation and flicker emissions. This issues have to be solved in order to comply with the grid code regulations.

An additional point of interest is to evaluate the smoothing effect that appears when the production of several WECs in a wind park is added. This effect may lead to lower costs for storage and to a more constant energy production. An analysis of this effect can be performed by shifting the time series of a single WEC by certain time delays in order to represent the aggregation effect for a given wave park, as a result an aggregation model is obtained.

The purpose of this report is to study the collection network for a wave energy park. The life-cycle cost for this collection system comprising investment and loss cost is to be made and an optimum, based on the wave energy distribution, is to be found. Moreover, a target is to determine the power quality impact of this farm. The LCC calculation is limited to the collection grid only, the wave energy units themselves are not included in this present study.

2. Theory

In this chapter, the theory related to the analysis performed is described.

2.1 Modelling

Cables can be modeled as an impedance Z

$$Z = R + jX \tag{1}$$

where R is the resistance and X is the reactance of the cable. The reactance X can be inductive X_L or capacitive X_C according to

$$jX_L = jwL, \quad -jX_C = \frac{-1}{jwC} \tag{2}$$

where L is the inductance of the cable, C is the capacitance and w is the electrical frequency. The π-model of the cable combines these elements in the form depicted in Fig 2.1.

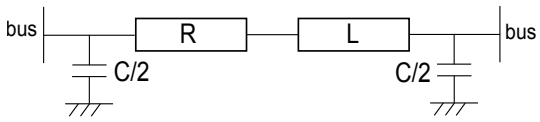

Figure 2.1: Cable π-model

The transformer model can be simplified as an impedance Z_t with a transformer ratio t_r

$$t_r = \frac{V_1}{V_2} \tag{3}$$

where V_1 and V_2 are the primary and secondary voltages respectively. The transformer parameters are computed as

$$Z = \frac{V_k U}{I}, \quad R = \frac{P_k}{3I^2} \tag{4}$$

$$X = \sqrt{Z^2 - R^2} \tag{5}$$

where P_k is the full-load copper loss and V_k is the voltage drop percentage. For power flow analysis admittances (Y) are used instead of impedances

$$Y = \frac{1}{Z} \tag{6}$$

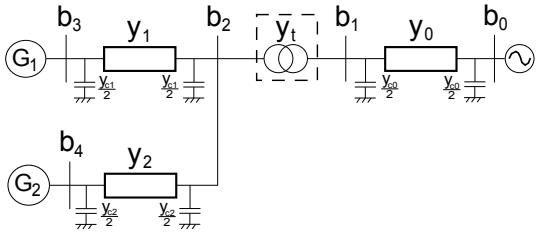

Figure 2.2: Meshed grid example using admittances

An example of use of admittances and the π-model of the cable is shown in Fig 2.2.

The small meshed grid used in the example can be expressed in an admittance matrix yielding (7) where the interconnection of the different buses is represented.

$$Y = \begin{bmatrix} y_0 + \frac{y_{c0}}{2} & -y_0 & 0 & 0 & 0 \\ -y_0 & t_r^2 y_t + y_0 + \frac{y_{c0}}{2} & -t_r y_t & 0 & 0 \\ 0 & -t_r y_t & y_t + y_1 + y_2 + \frac{y_{c1}}{2} + \frac{y_{c2}}{2} & -y_1 & -y_2 \\ 0 & 0 & -y_1 & y_1 + \frac{y_{c1}}{2} & 0 \\ 0 & 0 & -y_2 & 0 & y_2 + \frac{y_{c2}}{2} \end{bmatrix} \tag{7}$$

The voltages (U) and currents (I) in the nodes of the grid are related according to

$$I = YU \tag{8}$$

and the power flowing between the nodes can be determined as

$$S = P + jQ = UI^* \tag{9}$$

where S is the apparent power, P is the active power and Q is the reactive power.

2.2 Solution methodology

The voltage at each node and the power flowing through the cables can be computed using iterative methods. When solving the system, the convergence is determined using a tolerance (ϵ) that limits the minimum variation of the voltages norm, this tolerance bounds the accuracy of the solution.

$$\epsilon > \sqrt{\sum_{i=2}^{n} \Delta V_i^2} \quad \Delta V = V_{h-1} - V_h \tag{10}$$

where V_i is the voltage at the node i, n is the number of nodes and h is the iteration number.

The reactive power due to the cable capacitance is computed as:

$$Q = \frac{U^2}{X_C}, \tag{11}$$

and the power loss in the cables due to the Joule effect is:

$$P_{loss} = R \cdot I^2 \tag{12}$$

2.3 Economical analysis

The Net Present Value (NPV) is computed as:

$$NPV(N) = \sum_{t=0}^{N} \frac{R_t}{(1+i)^t} \tag{13}$$

where R_t is the net cash flow, i is the interest rate, N is the number of years and t is the time of the cash flow.

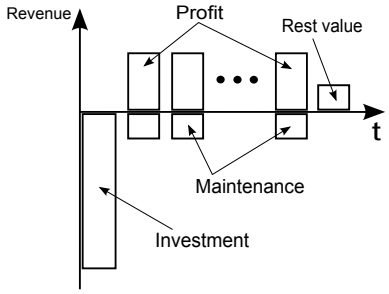

Figure 2.3: Net present value cash flow

The rest value R_v is computed as:

$$R_v = \frac{R_0}{(1+i)^t} \tag{14}$$

where R_0 is the initial investment and t is the last year of the cash flow analysis. In the case of life-cycle cost analysis all costs along the installation life are considered at the end of the lifetime.

2.4 Flicker analysis

The flicker coefficients are computed from the voltage fluctuations caused by the wave energy park at the point of common connection when the wave farm is operating in steady-state. The standard IEC 61400-21 presents a methodology for flicker contribution analysis where the power collection grid is connected to a fictitious grid with a short-circuit apparent power ($S_{k,fic}$) of 50 times the rated apparent power of the wave farm. A schematic view of the fictitious grid is depicted in Fig. 2.4

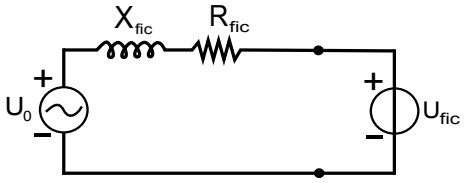

Figure 2.4: Fictitious grid for simulation of fictitious voltage

where U_0 is the instantaneous value of the voltage source and U_{fic} is the instantaneous value of the simulated voltage in the fictitious grid provided by this model.

The characteristics of the grid can be calculated by

$$S_{k,fic} = \frac{U_n^2}{\sqrt{R_{fic}^2 + X_{fic}^2}} \tag{15}$$

where U_n is the grid voltage and R_{fic} and X_{fic} are the fictitious grid resistance and reactance respectively. The ratio R/X is determined by the grid angle in the form

$$tan(\Psi_k) = \frac{X_{fic}}{R_{fic}} \tag{16}$$

where Ψ_k is the grid angle. The short term flicker emission values ($P_{st,fic}$) are evaluated for four grid angles $\Psi_k = \{30^o, 50^o, 70^o, 85^o\}$ using 10 minutes time-series measured with a cut-off frequency of at least 400 Hz. Then, the flicker coefficient values (c) can be computed for each grid angle as

$$c(\Psi_k) = P_{st,fic}\frac{S_{k,fic}}{S_n} \tag{17}$$

The flicker coefficient (C_f) shall be determined as the 99th percentile of the weighted accumulated distribution of the flicker coefficient values. Add explanation about what the Cf means

3. Case set-up

The set-up consists of 10 clusters with 10 generators. The nominal power of each generator is 100 kW and its voltage is 690 V. The distance to the shore is 10 km, the grid voltage at the connection point is 30 kV and the frequency is 50 Hz. A schematic view of a cluster is shown in Fig. 3.1 where b_G represent the buses considered in the analysis and z_G the impedance of the cables. The cable lengths are L=(240,190,190,150,190,120,190,150,240,190) in meters.

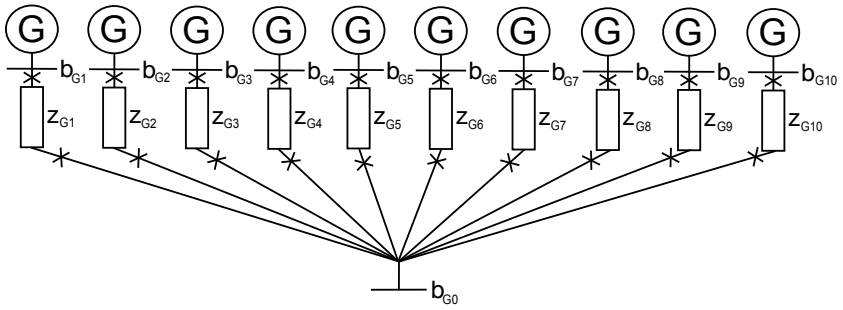

Figure 3.1: Cluster schematic view

3.1 Case 1

The first case under study (layout 1) is shown in Fig. 3.2, the voltage of the collection grid and the transmission cable is 30 kV. The bus b_{T0} corresponds to the grid connection point. The distance between clusters is 300m.

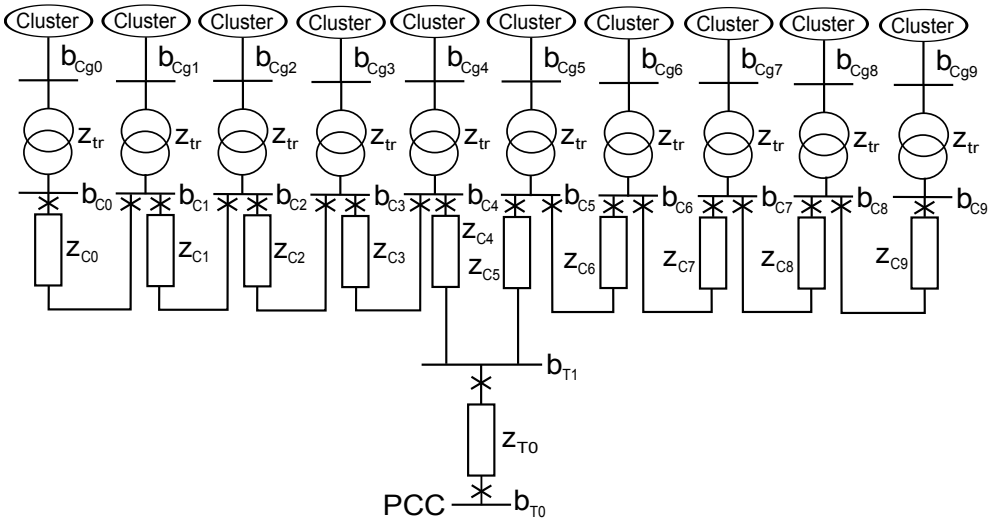

Figure 3.2: Layout 1 schematic view

3.2 Case 2

The second case under study (layout 2) is shown in Fig. 3.3, a redundant cable has been added increasing the reliability of the grid.

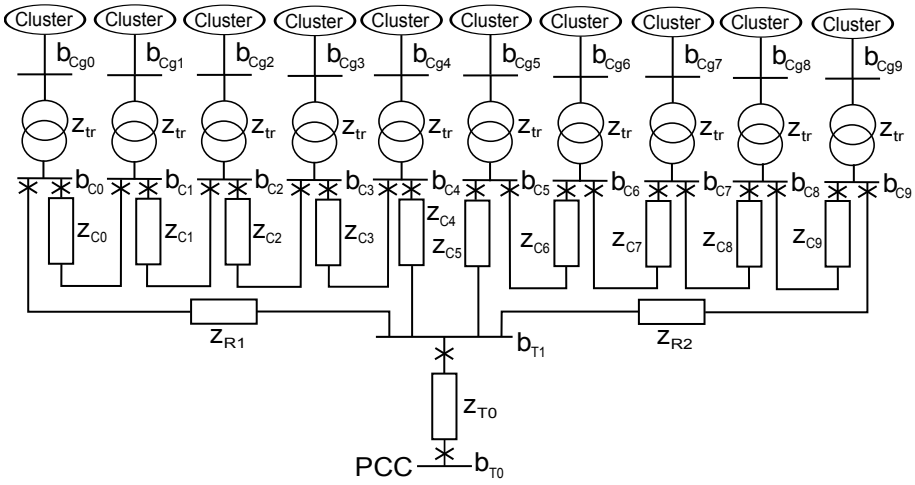

Figure 3.3: Layout 2 scheme. 30 kV collection grid.

3.3 Case 3

The third case under study (layout 3) is shown in Fig. 3.4, the collection grid has a voltage of 10 kV and the transmission is 30 kV. The voltage is increased in two steps in this layout.

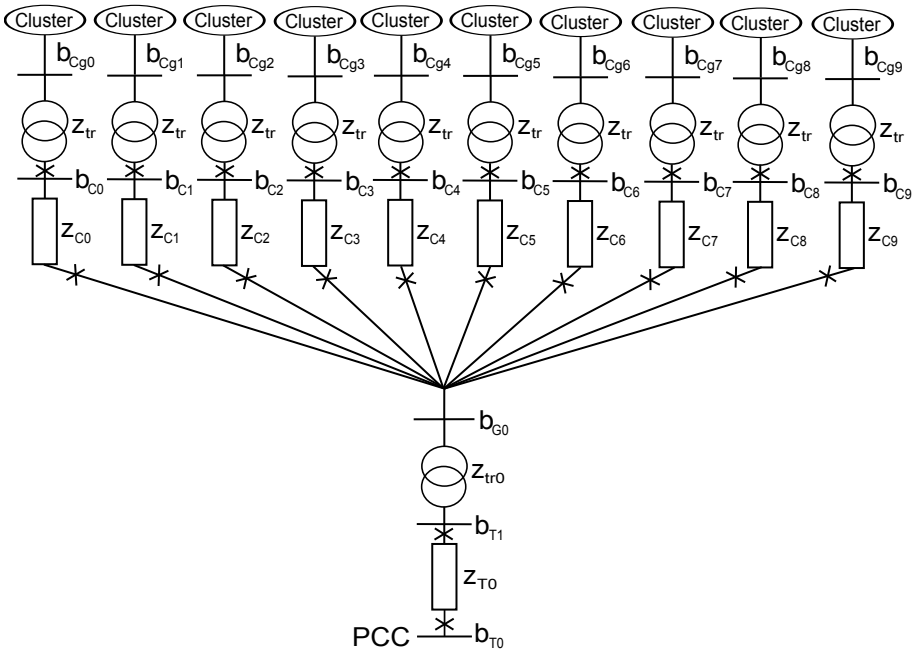

Figure 3.4: Layout 3 scheme. 10 kV collection grid and 30 kV transmission cable

4. Analysis

4.1 Cable parameters

The parameters obtained from [1] used for the analysis are listed below. Cluster cables:

- 1kV 50mm^2 cable: R=0.387 Ω/km, L=0.24 mH/km, c=0.5 μF/km, I_{rated}=175A.
- 1kV 70mm^2 cable: R=0.268 Ω/km, L=0.24 mH/km, c=0.54 μF/km, I_{rated}=210A.
- 1kV 95mm^2 cable: R=0.193 Ω/km, L=0.24 mH/km, c=0.56 μF/km, I_{rated}=250A.
- 1kV 150mm^2 cable: R=0.124 Ω/km, L=0.22 mH/km, c=0.58 μF/km, I_{rated}=315A.
- 1kV 240mm^2 cable: R=0.0754 Ω/km, L=0.22 mH/km, c=0.60 μF/km, I_{rated}=410A.

Collection grid cables:

- 10kV 50mm^2 cable: R=0.387 Ω/km, L=0.36 mH/km, c=0.28 μF/km, I_{rated}=175A.
- 10kV 70mm^2 cable: R=0.268 Ω/km, L=0.33 mH/km, c=0.29 μF/km, I_{rated}=210A.
- 10kV 95mm^2 cable: R=0.193 Ω/km, L=0.31 mH/km, c=0.33 μF/km, I_{rated}=250A.
- 10kV 150mm^2 cable: R=0.124 Ω/km, L=0.29 mH/km, c=0.39 μF/km, I_{rated}=315A.
- 10kV 240mm^2 cable: R=0.0754 Ω/km, L=0.28 mH/km, c=0.48 μF/km, I_{rated}=410A.

- 30kV 95mm^2 cable: R=0.193 Ω/km, L=0.38 mH/km, c=0.17 μF/km, I_{rated}=250A.
- 30kV 120mm^2 cable: R=0.153 Ω/km, L=0.37 mH/km, c=0.18 μF/km, I_{rated}=285A.
- 30kV 150mm^2 cable: R=0.124 Ω/km, L=0.36 mH/km, c=0.20 μF/km, I_{rated}=315A.

Transmission cables:

- 30kV 185mm^2 cable: R=0.0991 Ω/km, L=0.38 mH/km, c=0.21 μF/km, I_{rated}=355A.
- 30kV 240mm^2 cable: R=0.0754 Ω/km, L=0.37 mH/km, c=0.23 μF/km, I_{rated}=410A.
- 30kV 300mm^2 cable: R=0.0601 Ω/km, L=0.36 mH/km, c=0.25 μF/km, I_{rated}=460A.
- 30kV 400mm^2 cable: R=0.0470 Ω/km, L=0.35 mH/km, c=0.28 μF/km, I_{rated}=515A.
- 30kV 500mm^2 cable: R=0.0366 Ω/km, L=0.33 mH/km, c=0.31 μF/km, I_{rated}=580A.
- 30kV 630mm^2 cable: R=0.0283 Ω/km, L=0.32 mH/km, c=0.34 μF/km, I_{rated}=640A.

Transformer parameters:

- Transformer, 1000 kVA, 0.69/30 kV: R=0.0062 Ω, X=0.0279 Ω, $\varepsilon = 98.7\%$.
- Transformer, 1000 kVA, 0.69/10 kV: R=0.0045 Ω, X=0.0282 Ω, $\varepsilon = 99\%$.
- Transformer, 10 MVA, 10/30 kV: R=0.038 Ω, X=0.8341 Ω, $\varepsilon = 99.6\%$.

4.2 Components costs

The net present value is used for the economic evaluation of the layouts. The costs considered for the analysis have been obtained from [2], [8] and are shown in Table 4.1. The overall cost of generators, converters, platforms, communications and control systems is considered to be 42.6 MSEK for the entire park, this cost will be shared by all layouts included in this study. The prices marked with (i) have been interpolated from the EBR pricelist from Svensk Energi.

Table 4.1: Costs table

Item	Cost (kSEK)
Cable 50 mm^2 690 V (km)	56.1
Cable 70 mm^2 690 V (km)	73.6 (i)
Cable 95 mm^2 690 V (km)	95.5
Cable 150 mm^2 690 V (km)	163
Cable 240 mm^2 690 V (km)	210
Cable 10 kV 50 mm^2 (km)	191
Cable 10 kV 70 mm^2 (km)	207 (i)
Cable 10 kV 95 mm^2 (km)	227
Cable 10 kV 150 mm^2 (km)	284
Cable 10 kV 240 mm^2 (km)	367
Cable 30 kV 95 mm^2 (km)	287
Cable 30 kV 120 mm^2 (km)	318 (i)
Cable 30 kV 150 mm^2 (km)	356
Cable 30 kV 185 mm^2 (km)	385 (i)
Cable 30 kV 240 mm^2 (km)	430
Cable 30 kV 300 mm^2 (km)	453 (i)
Cable 30 kV 400 mm^2 (km)	495
Cable 30 kV 500 mm^2 (km)	560
Cable 30 kV 630 mm^2 (km)	621
Cable laying (km)	2400
Switchgear LV	102
Switchgear 10 kV	200
Switchgear 30 kV	371
Transformer 0.69/30 kV (1 MVA)	172
Transformer 0.69/10 kV (1 MVA)	172
Transformer 10/30 kV (10 MVA)	1810

- Maintenance: 1% of the investment (per year)
- Wholesale electricity price: 90 - 180 €/MWh (9 SEK = 1€)

4.3 Wave types

Three types of waves are considered in this study:

- H1: H_s=1.25 m, T_z=5.0 s
- H2: H_s=2.00 m, T_z=6.3 s
- H3: H_s=4.75 m, T_z=8.3 s

with H_s the height and T_z the period of the Pierson-Moskowitz spectrum of the waves. Time series of the power generated have been provided by OHT, being obtained from their simulation models for a scaled prototype. The power take-off using the gravity weight accumulator for the different wave types is plotted in Fig. 4.1. The simulated data has been multiplied with 5.4 to simulate a 100 kW unit.

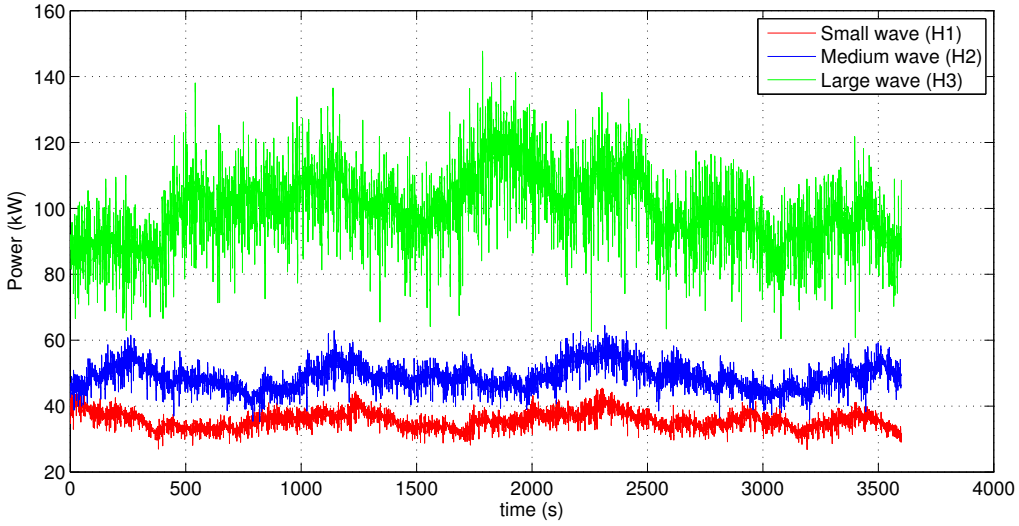

Figure 4.1: Smoothed power captured for different wave types (kW)

The average power captured is $P_{H1} = 35.88$ kW, $P_{H2} = 49.22$ kW, $P_{H3} = 100.57$ kW. The probability distribution of the waves is shown in Fig. 4.2.

Then, we can consider the following probability of occurrence for H1, H2 and H3 wave types

Table 4.2: Probability of occurrence

Wave type	Hs range (m)	Probability (%)
H1	0 - 1.25	49.6
H2	1.75 - 2.75	33.7
H3	3.25 - 8.75	16.7

4.4 Cables analysis

In the first stage of this study the size of the cables is chosen, the power losses and the cost of the cables will be used to achieve the proper selection. This analysis is divided in three parts where the

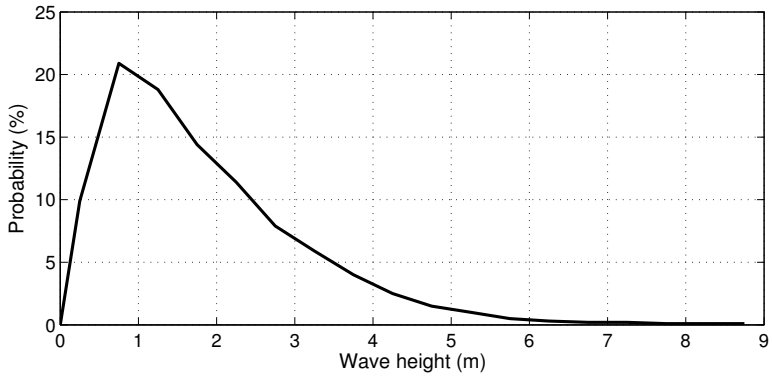

Figure 4.2: Probability distribution of waves

cluster, the transmission and the collection grid for each layout option will be considered separately. The components costs are obtained from the proposed EBR list which offers a wider range of choices, the prices for generator, converter, controller and platform are the ones suggested by OHT. The power losses cost are computed using an average energy price of 135 €/MWh. The interest ratio is 10% and the cash flow analysis is calculated over 20 years. Investment includes the initial investment and the maintenance cost during the life-cycle of the installation.

4.4.1 Cluster Analysis

The cluster layout is the same for all the cases in this study. The power loss for the different captured power and for each cable size is computed. Reactive power at the converters is regulated in order to have pf=1 at the PCC. The nominal current in the cluster is $I_{nom} = 83.7A$ with a voltage of 690 V. The resultant power losses in one cluster for the range of power generated is shown in Fig. 4.3.

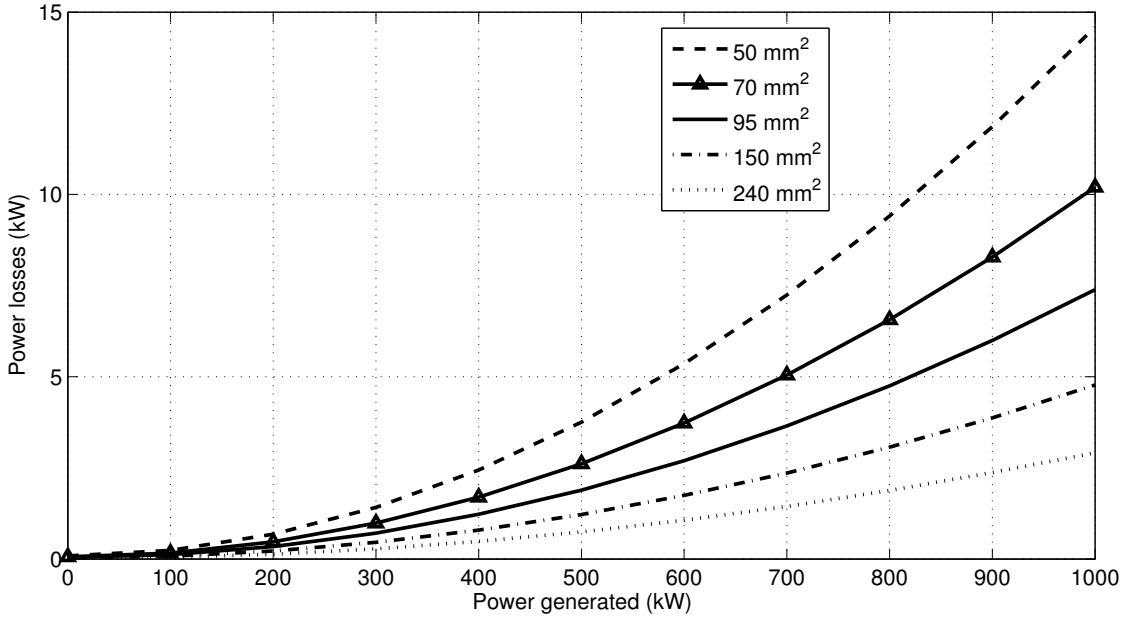

Figure 4.3: Power losses in one cluster for each cable size

Table 4.3: Power losses for different cable size in one cluster

	H1	H2	H3	Weighted average
$P_{generated}$ (kW)	35.88	49.22	100.57	51.18
P_{loss} $50mm^2$ (kW)	1.98	3.64	14.75	4.67
P_{loss} $70mm^2$ (kW)	1.38	2.53	10.31	3.26
P_{loss} $95mm^2$ (kW)	0.997	1.83	7.47	2.36
P_{loss} $150mm^2$ (kW)	0.642	1.18	4.83	1.52
P_{loss} $240mm^2$ (kW)	0.391	0.721	2.95	0.93

The average power generated and power losses will be used in the economical evaluation. We are now considering average generation for a period of 20 years and comparing income for each cable size. We consider that the cable length includes the distance from the device and the sea bottom (up and down). The results are summarized in Table 4.4.

Table 4.4: Cluster costs in MSEK

Section (mm^2)	Investment	Losses cost	Total cost
50	72.65	4.66	77.30
70	72.94	3.25	76.19
95	73.31	2.35	75.67
150	74.46	1.52	75.97
240	75.25	0.93	76.18

According to this analysis the cable with $95mm^2$ section should be used for internal cluster connection.

4.4.2 Transmission System Analysis

The distance to shore (10 km) is the same for all cases. Power loss for a range of active power and for each cable size is computed. Reactive power at the converters is regulated in order to have pf=1 at the PCC. The nominal current in the transmission cable is $I_{nom} = 192.5A$ and the voltage is 30 kV. The resultant power losses in the transmission cable for the range of power generated by the entire wave farm is shown in Fig. 4.4.

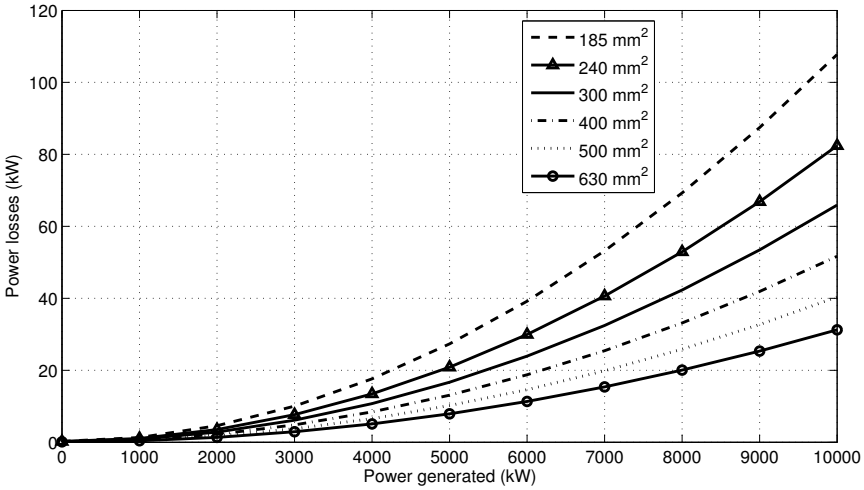

Figure 4.4: Power losses in the transmission to shorer for each cable size

Table 4.5: Power losses for different cable size

	H1	H2	H3	Weighted average
$P_{generated}$ (MW)	3.59	4.92	10.06	5.12
P_{loss} $185mm^2$ (kW)	14.23	26.50	108.99	34.19
P_{loss} $240mm^2$ (kW)	10.86	20.23	83.35	26.13
P_{loss} $300mm^2$ (kW)	8.69	16.17	66.65	20.89
P_{loss} $400mm^2$ (kW)	6.82	12.67	52.28	16.38
P_{loss} $500mm^2$ (kW)	5.32	9.89	40.80	12.79
P_{loss} $630mm^2$ (kW)	4.13	7.66	31.61	9.91

We are now considering average generation for a period of 20 years and compare profit for each cable size. We consider that the cable length includes the distance from the device and the sea bottom (up and down). The results are summarized in Table 4.6.

Table 4.6: Transmission costs in MSEK

Section (mm^2)	Investment	Losses cost	Total cost
185	34.86	3.41	38.27
240	35.15	2.60	37.76
300	35.30	2.08	37.38
400	35.57	1.63	37.21
500	35.99	1.28	37.27
630	36.39	0.99	37.38

According to this analysis the cable with $400mm^2$ section should be used for transmission to shore.

4.4.3 Collection Grid Analysis

4.4.3.1 Layout 1

In this layout the clusters are connected to each other. Reactive power at the converters is regulated in order to have pf=1 at the PCC. The voltage is 30 kV and the nominal current is $I_{nom} = 19.3A - 96.3A$ depending on the cable position. It should be noted that in case of cable failure a 10 % to 50 % of generation capacity will be lost. The resultant power losses in the collection grid for the range of power generated by the entire wave farm is shown in Fig. 4.5 and specified for each wave type in Table 4.7.

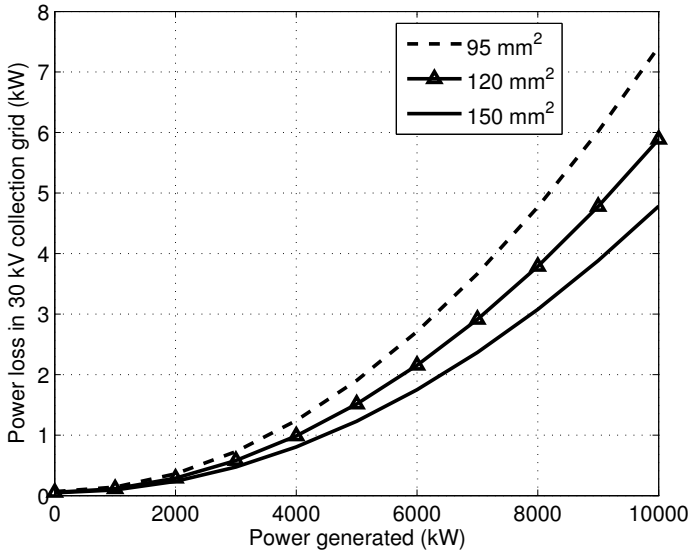

Figure 4.5: Power losses in the collection grid for each cable size

Table 4.7: Power losses for different cable size

	H1	H2	H3	Weighted average
$P_{captured}$ (MW)	3.59	4.92	10.06	5.12
P_{loss} $95mm^2$ (kW)	0.97	1.80	7.44	2.33
P_{loss} $120mm^2$ (kW)	0.77	1.42	5.90	1.84
P_{loss} $150mm^2$ (kW)	0.62	1.15	4.78	1.50

The power losses at the point of maximum generation (P=10MW) are: P_{95} = 7.4 kW, P_{120} = 5.9 kW and P_{150} = 4.8 kW. We are now considering average generation for a period of 20 years and compare profit for each cable size. The cable length includes the distance from the platforms and the sea bottom (up and down). The results are summarized in Table 4.8.

Table 4.8: Collection grid costs in MSEK

Section (mm^2)	Investment	Losses cost	Total cost
95	18.74	0.23	18.98
120	18.86	0.18	19.05
150	19.01	0.15	19.16

According to this analysis the cable with $95mm^2$ section should be used for collection grid connection.

4.4.3.2 Layout 2

In this case layout 1 is used again but a redundancy cable is included. Reactive power at the converters is regulated in order to have pf=1 at the PCC. The voltage is 30 kV and the nominal current in the transmission cable is $I_{nom} = 9.6A - 48.1A$ depending on the cable position. This layout increases reliability since a problem in any cable will not result in losing generation capacity. The resultant power losses in the collection grid for the range of power generated by the entire wave farm is shown in Fig. 4.6 and specified for each wave type in Table 4.9.

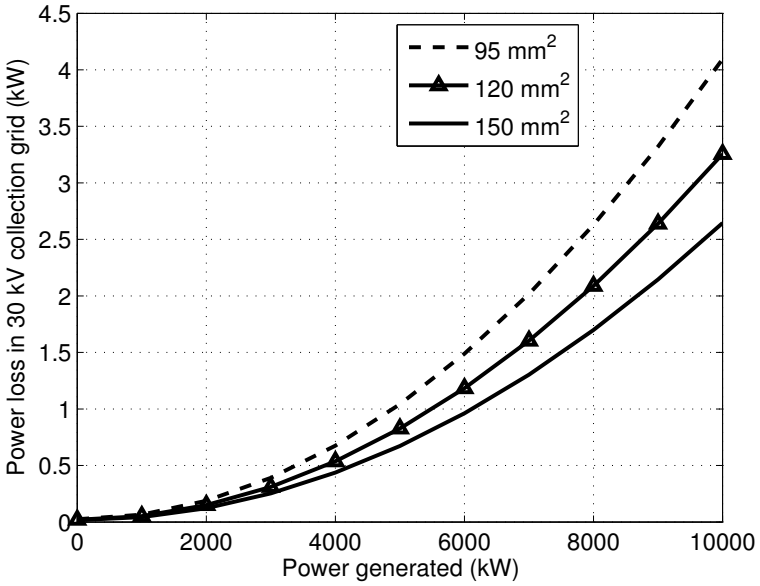

Figure 4.6: Power losses in the collection grid for each cable size

Table 4.9: Power losses for different cable size

	H1	H2	H3	Weighted average
$P_{captured}$ (MW)	3.59	4.92	10.06	5.12
P_{loss} $95mm^2$ (kW)	0.53	0.99	4.10	1.28
P_{loss} $120mm^2$ (kW)	0.42	0.78	3.25	1.02
P_{loss} $150mm^2$ (kW)	0.34	0.64	2.63	0.83

The power losses at the point of maximum generation (P=10MW) are: $P_{95} = 4.1$ kW, $P_{120} = 3.3$ kW and $P_{150} = 2.6$ kW. We are now considering maximum generation for a period of 20 years and compare profit for each cable size. The cable length includes the distance from the platforms and the sea bottom (up and down). The results are summarized in Table 4.10.

Table 4.10: Collection grid costs in MSEK

Section (mm^2)	Investment	Losses cost	Total cost
95	19.40	0.13	19.52
120	19.50	0.10	19.60
150	19.64	0.08	19.72

According to this analysis the cable with $95mm^2$ section should be used for collection grid connection.

4.4.3.3 Layout 3

In this layout the clusters are connected directly to the 10/30 kV step-up transformer. Reactive power at the converters is regulated in order to have pf=1 at the PCC. The voltage is 10 kV and the nominal current in the collection grid is $I_{nom} = 57.7A$. In case of cable failure a 10 % of generation capacity will be lost. The resultant power losses in the collection grid for the range of power generated by the entire wave farm is shown in Fig. 4.7 and specified for each wave type in Table 4.11.

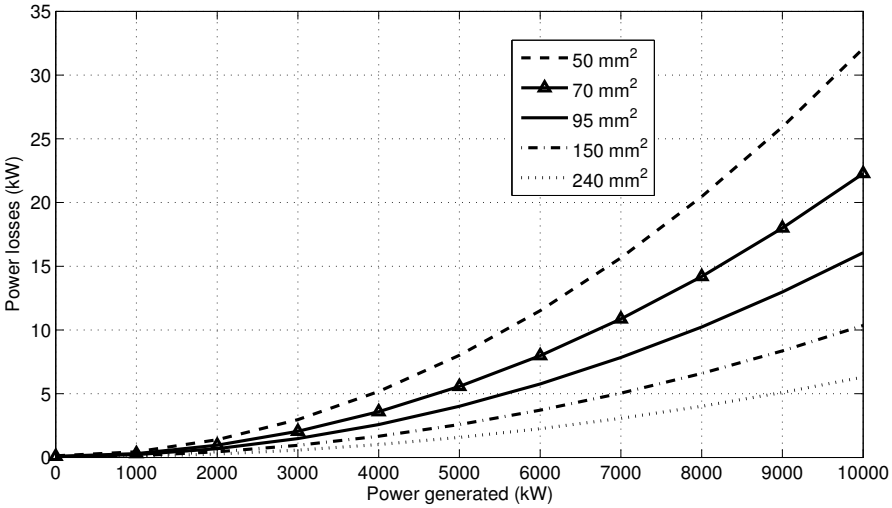

Figure 4.7: Power losses in the collection grid for each cable size

Table 4.11: Power losses for different cable size

	H1	H2	H3	Weighted average
$P_{captured}$ (MW)	3.59	4.92	10.06	5.12
P_{loss} $50mm^2$ (kW)	4.19	7.77	32.45	10.12
P_{loss} $70mm^2$ (kW)	2.90	5.40	22.53	7.02
P_{loss} $95mm^2$ (kW)	2.09	3.89	16.25	5.06
P_{loss} $150mm^2$ (kW)	1.35	2.50	10.48	3.26
P_{loss} $240mm^2$ (kW)	0.82	1.52	6.38	1.98

We are now considering average generation for a period of 20 years and compare profit for each cable size. The cable length includes the distance from the platforms and the sea bottom (up and down). The results are summarized in Table 4.12.

Table 4.12: Collection grid costs in MSEK

Section (mm^2)	Investment	Losses cost	Total cost
50	28.71	1.01	29.72
70	28.85	0.70	29.55
95	29.04	0.50	29.54
150	29.55	0.33	29.88
240	30.30	0.20	30.50

According to this analysis the cable with $95mm^2$ section should be used for collection grid connection.

4.4.4 Layouts Analysis

The power losses for each layout are now computed using the cable selection resulting from the previous analysis. The result for the range of power generated is shown in Fig. 4.8 and specified for each layout in Table 4.13.

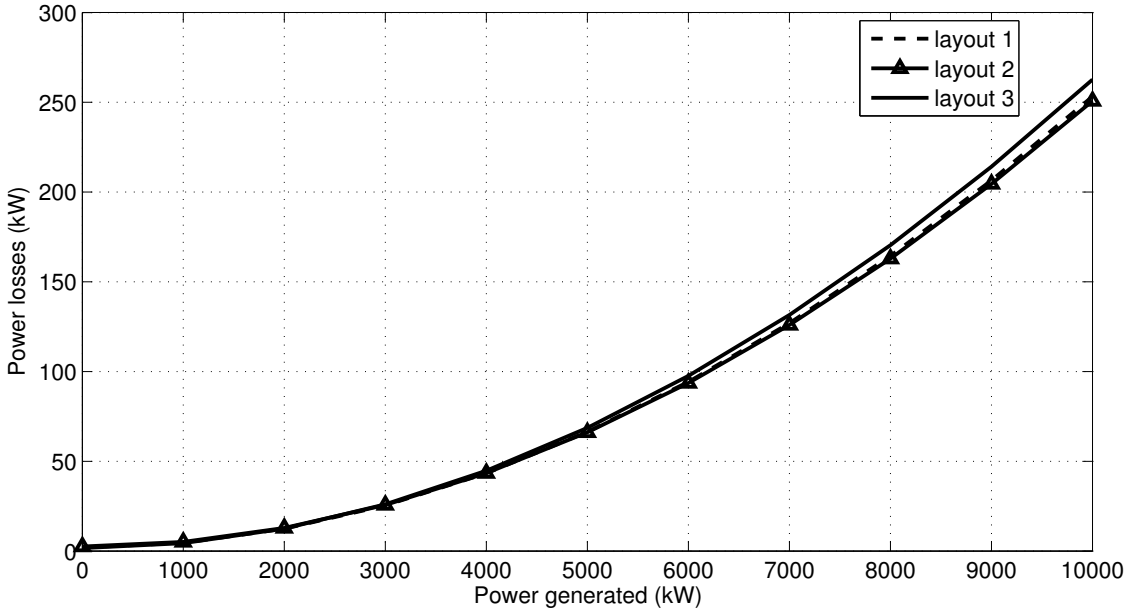

Figure 4.8: Power losses for each layout

Table 4.13: Power losses for different layouts

	H1	H2	H3	Weighted average
$P_{generated}$ (MW)	3.59	4.92	10.06	5.12
P_{loss} layout 1 (kW)	35.35	64.39	256.05	81.99
P_{loss} layout 2 (kW)	35.48	64.16	253.51	81.56
P_{loss} layout 3 (kW)	36.37	66.55	265.55	84.81

4.4.5 Electricity price

We are now considering average generation for a period of 20 years and compare profit for each cable size. Two scenarios depending on the electricity price are considered, in the first scenario the price is 90€/MWh and in the second is 180€/MWh. The results of this analysis are shown in Fig. 4.9, as can be seen the best option for both scenarios is the same, layout 1. The electricity price has a strong influence on the final revenue and economical viability of the project, however its influence is barely noticeable in the layout selection. That is because of the small difference in terms of power loss between layouts (less than 3 kW) which is a small percentage of the total power generated.

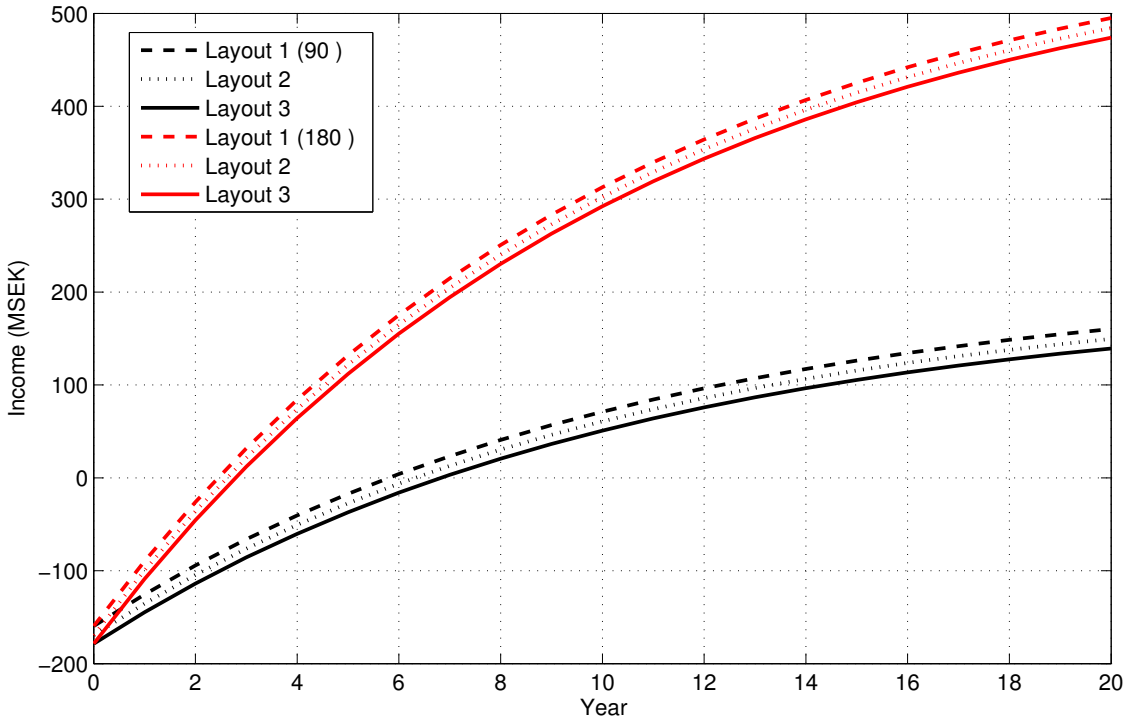

Figure 4.9: Layouts net present value. In red line the electricity price is 180€/MWh and in black line is 90€/MWh.

Table 4.14: Layout NPV analysis results in MSEK

Layout	Investment	Losses cost	Total cost	Income	Income - Grid cost
1 (90€)	174.53	5.49	179.98	334.77	160.25
2 (90€)	185.30	5.42	190.72	334.80	149.50
3 (90€)	195.29	5.64	200.93	334.59	139.30
1 (180€)	174.53	10.90	185.43	669.55	495.02
2 (180€)	185.30	10.84	196.14	669.61	484.30
3 (180€)	195.29	11.27	206.56	668.17	473.88

According to this analysis layout 1 should be selected. However, it should be remarked that layout 1 has less reliability and the possibility of losing generation capacity is not included in this analysis.

4.4.6 Failure time

We consider the case of a failure in layout 1 where the cable z_{c4} from bus b_{c4} in Fig. 3.2 is disconnected. In this situation, half of the power generated is lost. This failure situation is compared with layout 2 where losing a cable does not reduce the capacity to export power. The income difference between these two layouts is

$$R_{diff} = R_{layout1} - R_{layout2} = 10.73 \text{ MSEK}. \tag{1}$$

The power lost after the failure is half of the average power delivered, that is

$$P_{lossfail} = \frac{5118 - 81.99}{2} = 2518 \text{ kW}. \tag{2}$$

Considering an average energy price (135€/MWh) we have a profit loss of $Prof_{loss} = 339.93$ €/h. The evolution of the difference in income between layout 1 and layout 2 (R_{diff}) when the cable z_{c4} is failing is shown in Fig. 4.10. In this plot, the income difference decreases when the failure time increases.

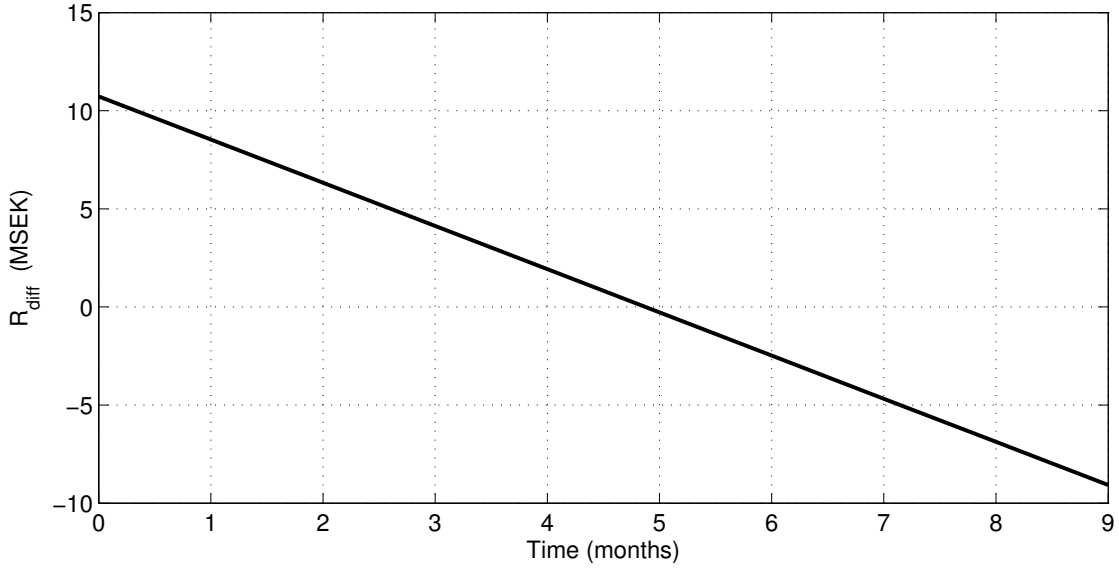

Figure 4.10: Income difference evolution

Now we can compute how long the failure can last in layout 1 until layout 2 becomes more profitable

$$t_{fail} = \frac{R_{diff}}{Prof_{loss}} = 3507 \text{ hours}, \tag{3}$$

that is 4.87 months. If the down time while replacing the cable is longer than the resulting failure time, layout 2 should be used instead of layout 1. The probability of failure of each component should be considered to weight the possible power loss. Only the grid collection cables will have an impact in this calculations since the rest of the elements are common for both topologies, neither the cost of replacing the cable (except for the redundant cable) will have an effect because it will be the same for both cases.

4.4.7 Interest rate analysis

In this section three interest rates are considered, 5, 10 and 15 %. Its influence on the layout selection and the revenue is studied considering an average electricity price of 135€/MWh, the results are summarized in Table 4.15 and plotted in Fig. 4.11. The results show that there is very little influence regarding layout selection, nevertheless it is an important factor in terms of final revenue.

Table 4.15: Layout net present value analysis for different interest rate in MSEK

Layout	Interest ratio	Investment	Total cost	Income - Grid cost
1	5%	180.47	188.08	287.30
2	5%	191.61	199.18	276.20
3	5%	201.93	209.81	265.58
1	10%	174.53	179.98	160.24
2	10%	185.30	190.72	149.50
3	10%	195.29	200.93	139.30
1	15%	171.07	175.26	86.25
2	15%	181.63	185.80	75.71
3	15%	191.42	195.75	65.76

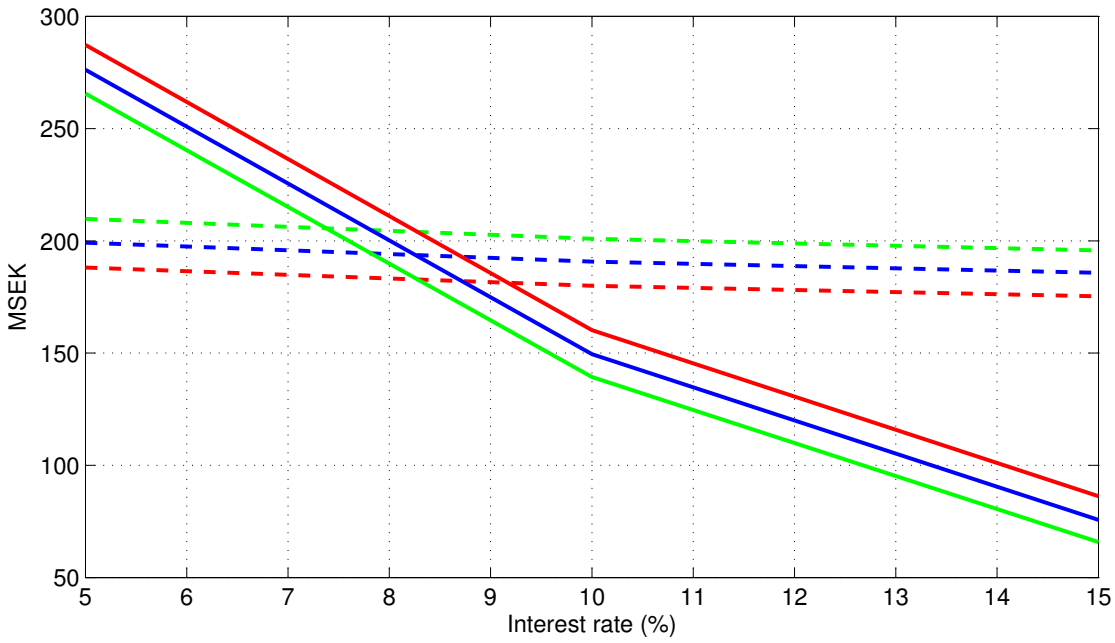

Figure 4.11: Layout net present value for different interest rates. Red - Layout 1, Blue - Layout 2, Green - Layout 3. Dashed - total cost, Solid -Income-Cost.

The total revenue after 20 years shows a clear decrease in Fig. 4.11 due to the increase of the interest rate, however the total cost (that includes investment and power losses cost) is barely affected.

4.4.8 Rest Value

After the period of exploitation of the wave farm the elements of the collection grid can be sold by a fraction of their initial value using (3). The analysis shown in Table 4.16 is performed considering 20 years and different interests rate.

Table 4.16: Rest value of each layout in MSEK

Interest rate	Layout 1	Layout 2	Layout 3
5%	60.15	63.86	67.30
10%	23.72	25.18	26.54
15%	9.75	10.35	10.91

4.5 Case 2 (proposal)

In order to repeat the analysis for 200 kW per wave unit we have to check if the layouts selected have capacity to transport the amount of power. In Table 4.17 we can see the current circulating through each section of the layout and the rated current of the selected cables. The worst case is selected for the 30 kV collection grid.

Table 4.17: Currents for each section of the layout in Amperes

Current (A)	$P_{gen} = 100$ kW	$P_{gen} = 200$ kW	Cable capacity
Cluster cable (95 mm^2)	83.67	167.35	250
30 kV collection grid (95 mm^2) (5 MW)	96.23	192.45	250
10 kV collection grid (95 mm^2) (1 MW)	57.73	115.47	250
Transmission cable (400 mm^2)	192.45	384.90	515

The net present value analysis, considering an average electricity price of 135€/MWh and an interest rate of 10%, is shown in Table 4.18.

Table 4.18: Layout net present value in MSEK

Layout	Investment	Losses cost	Total cost	Income	Income - Grid cost
Layout 1	174.53	31.00	205.53	989.67	815.14
Layout 2	185.30	30.69	215.99	989.98	804.68
Layout 3	195.29	32.14	227.42	988.53	793.24

Layout 1 results to be also the best option for 200 kW wave energy units.

5. Grid code compliance

Grid code compliance is studied against 100 units of 100 kW each moving simultaneously as being obtained from simulation models, with time series provided by OHT as described in Section 4.3. This model will later in the study be referred to as the single model. Table 5.1 summarizes the requirements of the grid code [3] for a small power plant connection.

Table 5.1: Grid code requirements

	Requirements	Calculations
Voltage level	± 10 %	Ok
Power factor	0.95 lag to 0.95 lead	Ok
Frequency operation	47 to 52 Hz	Ok
Harmonics	THD $\leq$ 3% at HV	Ok
LVRT	Reactive current infeed	Requirements must be put on wave energy units
Flicker (IEC)	P_{st} =0.3 unit P_{lt}=0.2 unit	Ok

It should be remarked that, according to the UK grid code the flicker limits are $P_{st} = 1.0$, $P_{lt} = 0.8$ but these values are not based on the IEC standard. In order to perform the analysis the parameters of the Utgrunden grid will be used, the characteristics of this grid are:

- Grid voltage: $U_{grid} = 55$ kV
- Short-circuit impedance: $S_k = 126$ MVA
- Grid angle: $\Psi = 73^{o}$

With this information we can compute the parameters:

$$Z = \frac{U_{grid}^2}{S_k}, \quad R = Zcos(\Psi), \quad X = Zsin(\Psi) \tag{1}$$

Although it will be considered a 30 kV grid at the connection point of the wave farm.

5.1 Voltage level

The variation of the voltage level at the PCC is computed as,

$$\Delta V = RI + XI_c \tag{2}$$

The value of I_c corresponds to the reactive current at the PCC, in this analysis the converters do not generate reactive power to compensate. The results of the evolution of the voltage level are plotted in Fig 5.1, a wave type H3 has been used to obtain these results since it is the limit case. Voltages in per unit are referred to a base voltage, the base voltage of the PCC is referred to the transmission voltage (30kV) and the base voltage of the converter is 690 V. The actual voltage value can be computed using

$$V = V_{pu} \cdot V_{base} \tag{3}$$

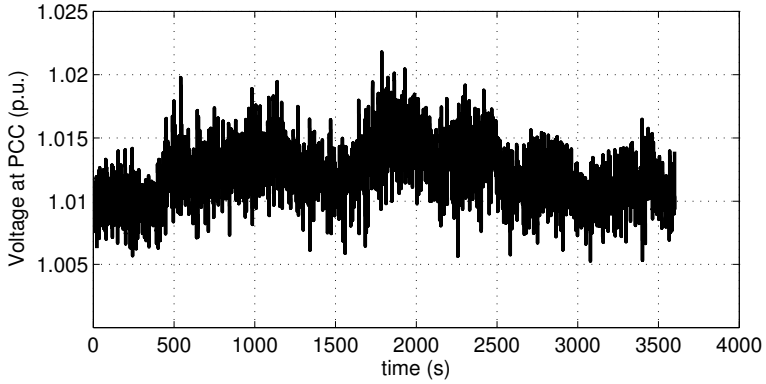

Figure 5.1: Voltage level at the PCC (no tap changer actions) in per unit (p.u.)

As can be seen during maximum generation the voltage level never exceeds the 1.1 p.u marked as a limit by the grid code. The voltage variation at the power converter is shown in Fig 5.2.

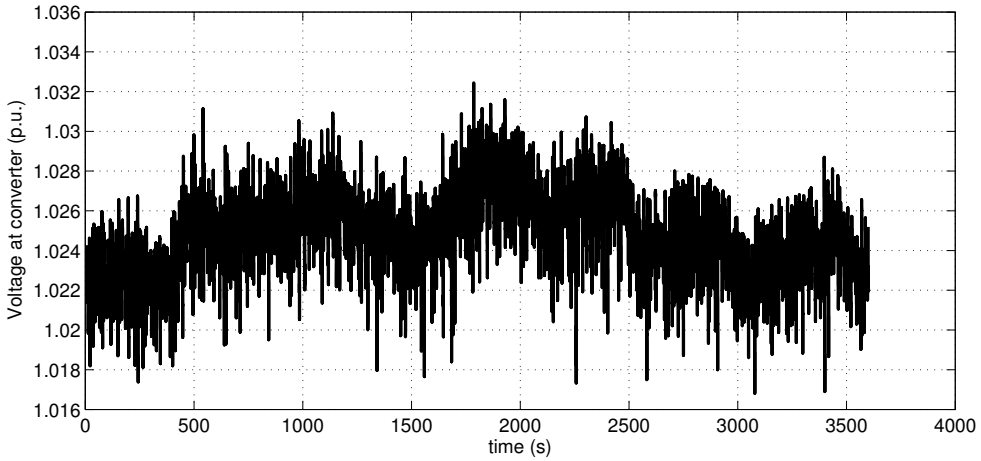

Figure 5.2: Voltage level at the power converter in per unit (p.u.)

5.2 Power Factor

The power factor at the PCC is computed as,

$$pf = \frac{P}{S} \tag{4}$$

which is the ratio between the real power delivered to the grid and the apparent power at the PCC. The results are plotted in Fig 5.3, in this analysis the converters do not generate reactive power. The worst case for this analysis is the wave type H1 since with this wave type there is less real power being generated.

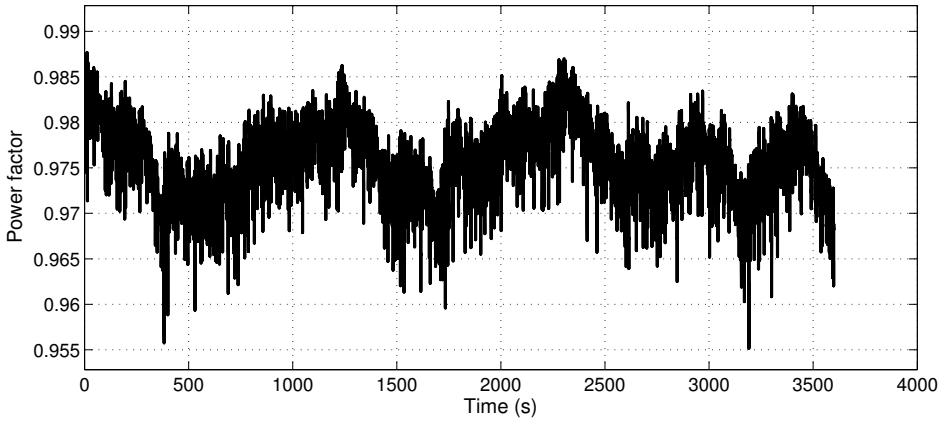

Figure 5.3: Power factor at the PCC for a wave type H1

According to [3] the limits of the power factor are reduced linearly with the amount of power plant in service when it is below 50% and above 20% of the nominal power, as shown in Fig 5.4. The red dots correspond to the location of the different wave types.

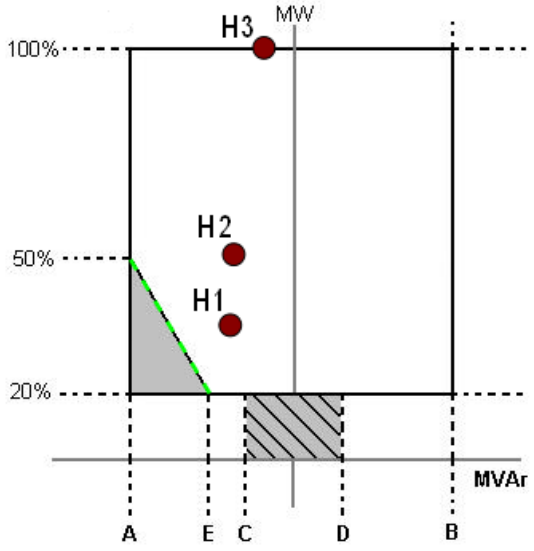

Figure 5.4: Reactive power limits

The power factor for a range of power generated by a wave energy unit is shown in Fig 5.5. It can be noticed that for generation levels below 25 kW per wave unit some reactive power will have to be supplied by the power converters to comply with the grid code requirements. The reduced limit (from point A to E in Fig 5.4) is marked in green line in Fig 5.5, according to the grid code the point E is equivalent (in MVAr) to a -12% of rated MW output.

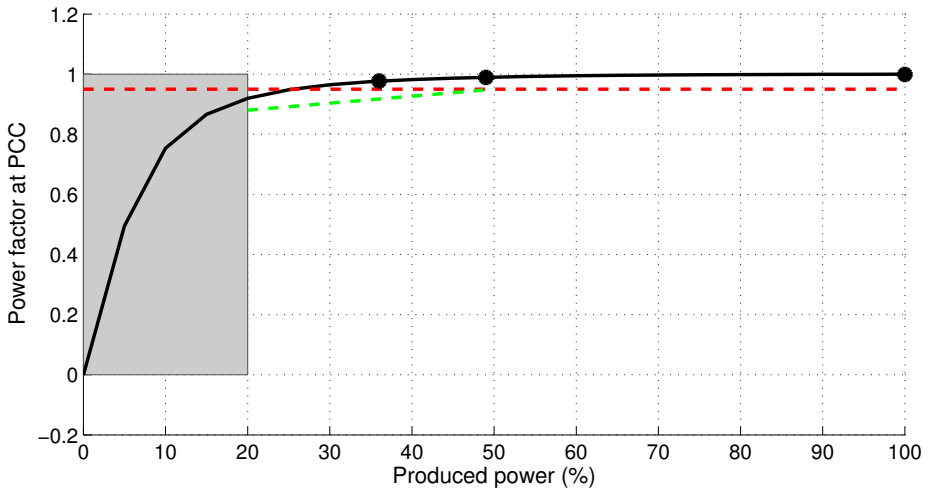

Figure 5.5: Power factor at the PCC for a range of power generated. In red dashed line there is marked the 0.95 power factor limit, the green line marks the reduced reactive power limit. The power factor corresponding to wave types H1, H2 and H3 are indicated by triangular marks

The amount of reactive power that has to be supplied by a power converter in order to have a unity power factor at the PCC for a range of real power is shown in Fig 5.6. It can be seen that reactive power between 8 and 9 kVAr will have to be supplied which is an acceptable value for a power converter with a rated power of 100 kVA.

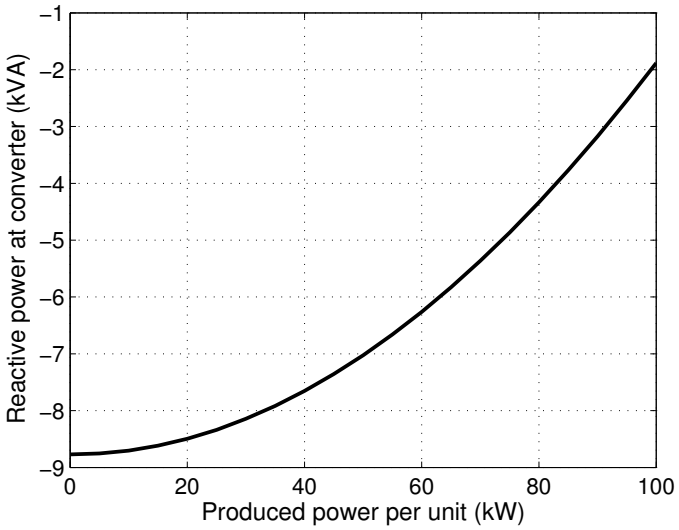

Figure 5.6: Reactive power injected by each converter

5.3 Low-Voltage Ride-Through

As stated in the grid code the generation unit must remain connected during the voltage drop above the line plotted in Fig. 5.7

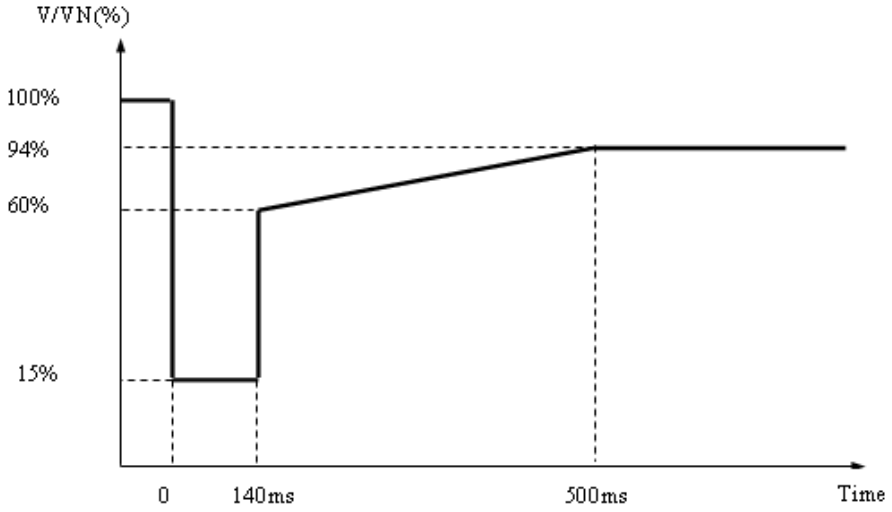

Figure 5.7: Voltage dip

where V/V_N is the retained voltage respect to the nominal voltage of the grid. If the voltage goes outside the area delimited by the solid line the wave farm will be allowed to trip and disconnect from the grid until the fault is cleared. During the fault it may be required to support the grid voltage supplying reactive power as an ancillary service. The amount of reactive power will be negotiated with the grid operator in a bilateral agreement, depending on the characteristics of the grid in the region where the power plant is operating this ancillary service can be more or less necessary.

During a voltage drop the amount of real power that can be evacuated is limited, in this situation the excess of power is dissipated in the DC-Chopper, a resistor located in the DC-link of the converter. The resistor should be dimensioned for the moment of maximum generation ($P = 100$ kW) and a voltage drop of 15%. In this situation $P_d = 85$ kW will have to be dissipated during $t = 140$ ms yielding a total energy of:

$$Energy = P_d \cdot t = 85000 \cdot 0.14 = 11900J \tag{5}$$

The thermal inertia of the resistor may allow to reduce the size of the DC-Chopper given the short time of the voltage drop.

5.4 Flicker

To perform a flicker analysis of the smoothed power, the measured data has been resampled to 256 Hz in order to apply the IEC 61400-21 procedure. A low-pass filter with a cut-off frequency of 10 Hz has been applied to eliminate the high-frequency noise resulting from the resampling process. In Fig. 5.8 the voltage fluctuation at the PCC is plotted, it corresponds to a grid with 50 times the short-circuit capacity of the wave farm and a grid angle of 30°.

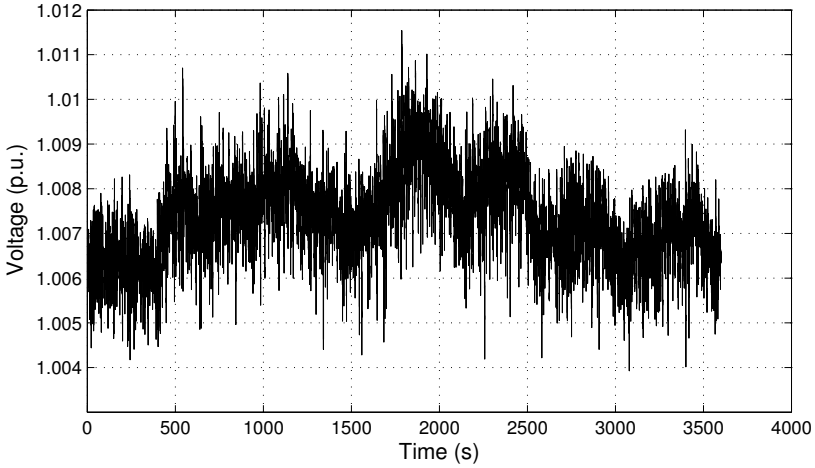

Figure 5.8: Resampled voltage fluctuation for grid angle of 30°

Table 5.2 summarizes the results of flicker coefficients for the wave farm. The coefficients are computed for different grid angles as is requested by the IEC standard 61400-21, instead of the 99th percentile the maximum coefficient is selected, the values obtained comply with the grid code requirements.

Table 5.2: Flicker coefficients

Ψ	P_{st}	C_f
30°	0.09	4.4
50°	0.07	3.6
70°	0.05	2.3
85°	0.02	1.2

5.4.1 Non-smoothed power

The voltage fluctuation at the PCC is shown in Fig. 5.9, in this case the non-smoothed power captured by the wave energy unit is used as power output for each generator. The characteristics of the grid are the same presented previously, 50 times the short-circuit capacity of the wave farm and a grid angle of 30°.

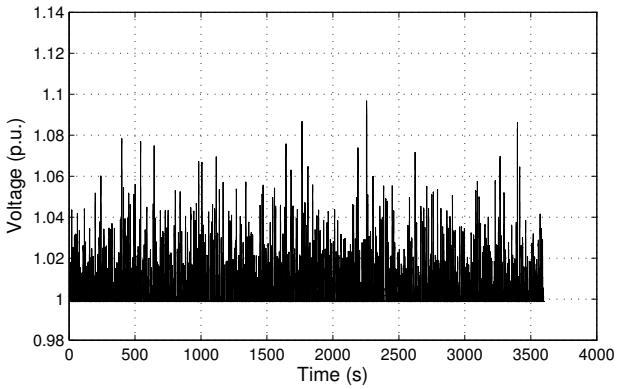

Figure 5.9: Resampled voltage fluctuation for grid angle of 30°

Before proceeding to compute the flicker coefficients a high frequency peak (shown in Fig. 5.10) has been removed since it distorted the resulting values.

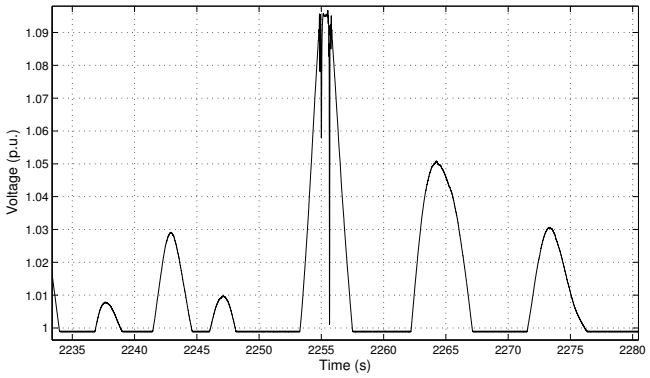

Figure 5.10: High frequency distortion in the sampled signal

The results of the flicker analysis for the captured power (before being filtered by the smoothing device) are shown in Table 5.3

Table 5.3: Flicker coefficients for non-smoothed power

Ψ	P_{st}	C_f
30°	0.67	33.5
50°	0.62	30.9
70°	0.51	25.5
85°	0.42	20.8

5.4.2 Aggregated model

An aggregated model of the wave power units has been simulated for two different cases. In the first case 10 units are moving simultaneously (i.e. the same wave is impacting them) and in groups of ten the wave park is randomly distributed (this model will be referred to as group model). In the second case every unit is moved randomly as individual waves are impacting them (this model is called park model). A flicker analysis has been performed for the data gathered using the smoothed and captured (non-smoothed) power. The results are summarized in Tables 5.4 and 5.5.

Table 5.4: Flicker coefficients using the smoothing device

Grid angle (Ψ)	30°	50°	70°	85°
Single model	4.4	3.6	2.3	1.2
Group model	1.5	1.2	0.8	0.4
Park model	0.5	0.4	0.3	0.2

Table 5.5: Flicker coefficients using the non-smoothed power

Grid angle (Ψ)	30°	50°	70°	85°
Single model	33.5	30.9	25.5	20.8
Group model	9.3	7.7	5.1	2.9
Park model	2.9	2.3	1.5	0.8

The flicker coefficients are reduced with respect to the less aggregated models. The maximum voltage variation for each model (single, group and park) at the PCC with a grid angle of 30° is shown in Table 5.6.

Table 5.6: Maximum voltage variation for each model in %

Model	Single	Group	Park
Smoothed power	1.2	1.0	0.86
Non-smoothed power	9.65	2.85	1.42

These tables should be considered tools that indicate the level of flicker emissions of the wave park but not the final result. They can be used as look-up tables to compute the short-term flicker emissions (P_{st}) of the power plant for a given AC grid connection point. Once the connection point is determined and the parameters (grid angle (Ψ) and grid short-circuit capacity (S_k)) are obtained it can be checked if the installation complies with the local grid code or not. The results are provided considering rated power (10 MW) and a wave park short-circuit capacity of 12 MVA (S_n). The parameters of the grid where the Utgrunden wind farm is connected are selected to provide an example of use of these tables. The grid angle is 73° in this point, if we consider the single model and the smoothed power we can see that the flicker coefficient will be around 2, then the flicker emissions are computed as

$$P_{st} = \frac{C_f \cdot S_n}{S_k} = \frac{2 \cdot 12}{126} = 0.2 \tag{6}$$

This value matches with result for the wave type H3 shown in Fig. 5.12 as expected, the wave park will comply with the regulations in this case. If the group model and the non-smoothed power are selected the flicker coefficient will be around 5, following the same procedure we will obtain $P_{st} = 0.5$ which exceeds the limits marked by the grid code and, therefore, the grid operator will not accept to connect the wave park to the grid in this point.

The reduction in the flicker coefficients from one model to another is due to the amplitude reduction of the voltage fluctuation. In order to check if the frequency of the voltage fluctuation is being displaced

by effect of the aggregation a Fast Fourier Transformation (FFT) is performed. The FFT yields the spectrum of the single model and the group model, the results are shown in Fig. 5.11 for the smoothed power. As can be observed the frequency spectrum remains almost unaltered from one model to the other.

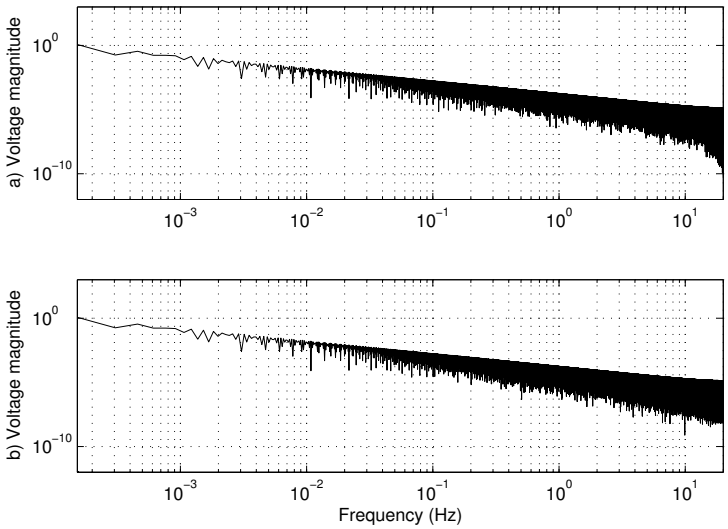

Figure 5.11: Smoothed power logarithmic frequency spectrum. a) Single model, b) Group model

5.4.3 Study case: Utgrunden reference network

For this analysis we will use the single model and a wave park of 100 units. The short term flicker emission values are computed using the short-circuit capacity of the Degerham switchgear station where the Utgrunden wind park is connected. The value are computed for different wave types and the results are plotted in Fig. 5.12. It can be observed that there is no problem regarding flicker emissions since the resulting coefficients fall well within the limits of the regulations.

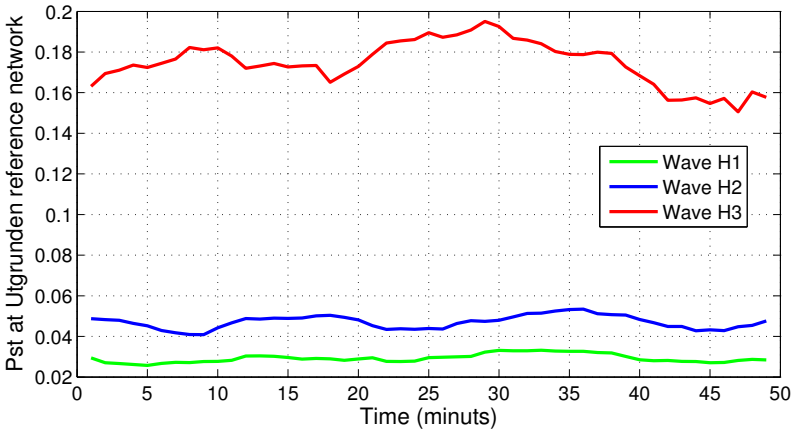

Figure 5.12: P_{st} values for each wave type

6. Grounding, transformer couplings and breaker location

The protection system of the collection grid should ensure the secure operation of its components and the correct protection for fault currents and lightnings. The distribution of breakers to isolate the line where the fault is located is shown in Fig. 6.1. The correct earthing of the installation is important to avoid dangerous overvoltages that can affect the proper functioning or reduce the lifetime of the components. This issue is also important in order to minimize the potential risk to human health during maintenance operations. An illustrative schematic view of the grounding system is sketched in Fig. 6.1 where the type and disposition of transformers is shown. The neutral point of the star side of the transformers is connected to the ground as depicted in the scheme.

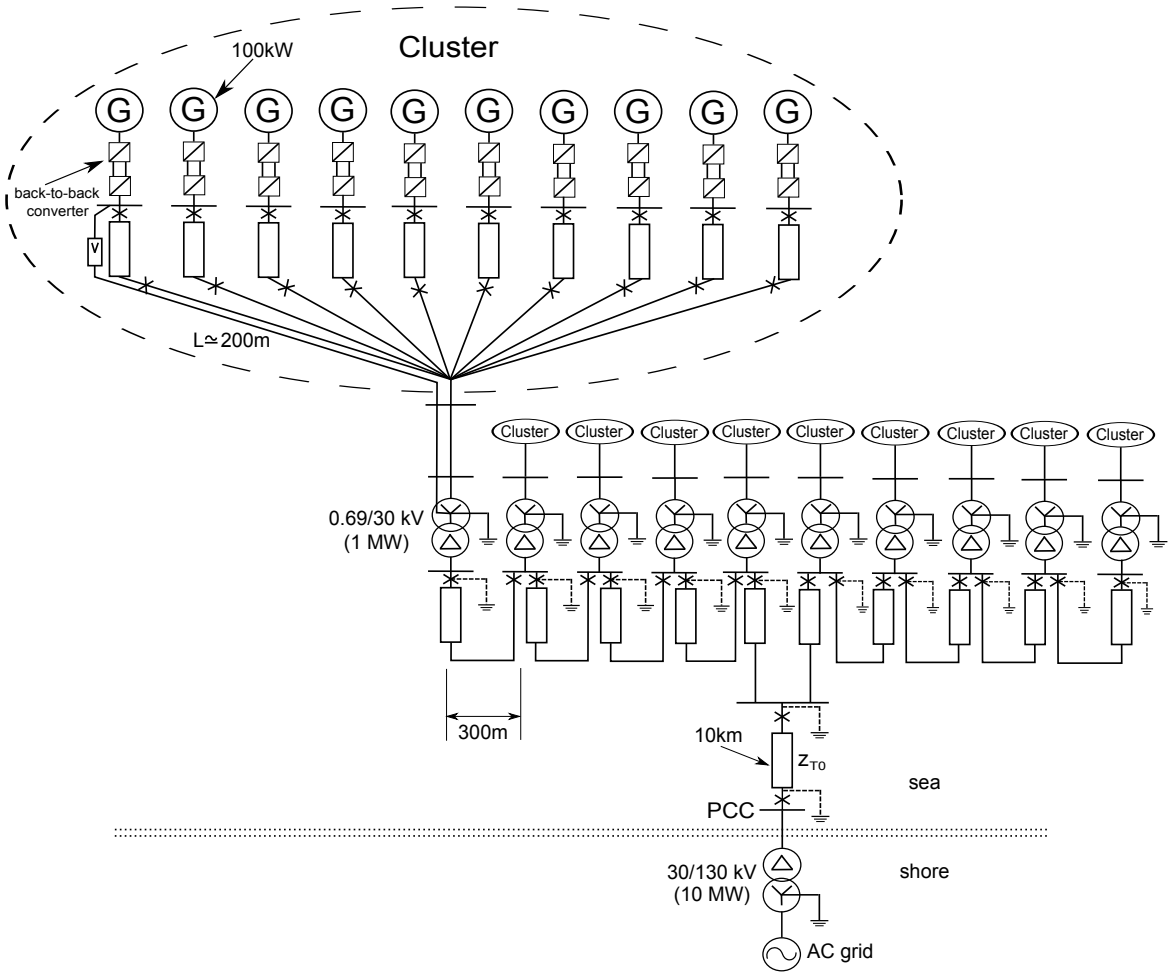

Figure 6.1: Collection grid design scheme

The medium voltage (30 kV) cables usually have a shield that should be grounded, short cables can be grounded in one end but if the cable is long it has to be grounded in both ends as shown in Fig. 6.1. In order to avoid circulating currents in the sheaths, minimize shield losses and reduce magnetic fields it is recommended the cross-bonding of cables where the shields are bonded together as depicted in Fig. 6.2.

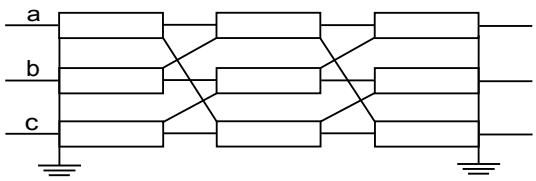

Figure 6.2: Cross-bonding of shields

7. Life-Cycle Cost for collection grid system

The Life-Cycle Cost (LCC) is defined as the sum of all costs incurred during the lifetime of an installation. The energy produced during the lifetime can be used to compute an estimation of the minimum energy price necessary to make the project profitable, this is computing the ratio LCC/energy (€/MWh).

To calculate the LCC the following aspects have to be considered:

- Lifetime (t): wave farm lifetime.
- Installation cost (IC): money invested to build the wave farm.
- Components cost (CC): components of the initial installation **(the wave energy unit is not included)**.
- Decommission cost (DC): includes cost of decommissioning and the return from the realization of the recycled material.
- Capital cost (Cap): loan amortisation.
- Maintenance (M): preventive and corrective maintenance (including storage and spare parts).
- Discount rate (DR): rate of return that could be earned on an investment in the financial market with similar risk.
- Loan interest (LI)
- Inflation rate (I)
- Energy production (EP): total energy production during the lifetime.
- Other costs: Insurance, Logistics, Project development, Permits... (these costs are not included).

The LCC can be computed then using the following expression:

$$\frac{LCC}{MWh} = \frac{IC + CC + \frac{DC}{(1+DR)^t} \sum_{i=1}^{t} \frac{Cap(i)LI + (1+I)^i M}{(1+DR)^i}}{EP} \tag{1}$$

The costs considered for this analysis are:

- Lifetime (t): 20 years.
- Installation cost (IC): 8.85 M€ (cable laying)
- Components cost (CC): 8.88 M€ (generator, converter, controller, transformers, cables, switchgears and platforms)

- Decommission cost (DC): 19.12 M€ (removal+disposal-return value)
- Capital cost (Cap): 0.89 M€ per year ($\frac{CC+IC}{t}$)
- Maintenance (M): 0.18 M€ per year (1% of (CC+IC))
- Discount rate (DR): 10%
- Loan interest (LI): 5%
- Inflation rate (I): 3%
- Energy production (EP): 44133 MWh

Decommission costs are obtained from [6] being 679.3€/m for removal costs and 307.2€/ton for disposal costs. As a result we find out that to cover the collection grid cost an electricity price share of 30.8€/MWh is needed. Based on the assumptions presented above the cost share of each concept is obtained and shown in Fig. 7.1 and Table 7.1.

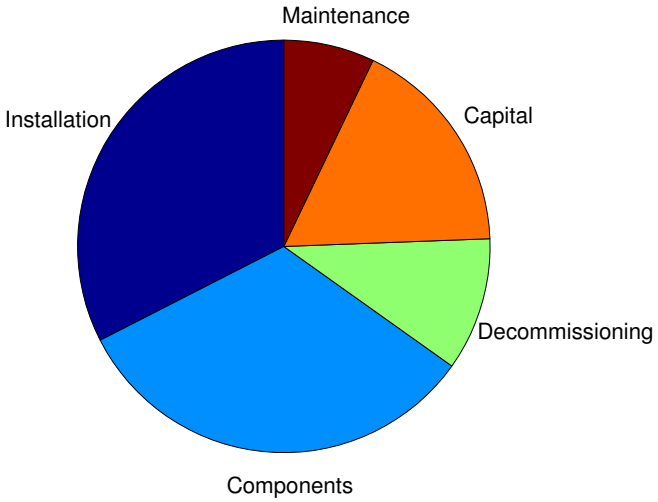

Figure 7.1: Life-Cycle cost analysis

Table 7.1: Life-Cycle cost results based on the assumptions presented in the study

Cost	Installation	Components	Decommissioning	Capital	Maintenance
Percentage (%)	32.5	32.6	10.4	17.2	7.1

8. Conclusions

The collection grid is designed using a trade-off between cost and power loss, a weighted average power production taking into account the probability distribution of the sea state and the maximum production for minimum size of the cables that are used in this design. This study yields that three-core cables with a copper conductor with a cross section of 95 mm^2 and 690 V isolation should be used for cabling the wave energy units inside the clusters, also 95 mm^2 with 30 kV isolation for interconnection of clusters and a section of 400 mm^2 with 30 kV for the transmission cable to shore.

Three layouts are compared, in one, two voltage step-up levels are used (layout 3) and in the other two only one voltage level is considered (layouts 1 and 2), the results show that one voltage step-up is more profitable, the increase of investment in transformers do not yield enough reduction in cabling cost to become economically interesting. Redundancies are also studied between layouts 1 and 2 and an analysis of the worst case of failure time is done. This analysis show that a failure in the most critical cable in layout 1 would need a down time of more than 4 months to match the results of layout 2, any other failure will just increase the down time required to equalize both layouts. This result does not justify the selection of layout 2, instead layout 1 is chosen as the collection grid for further analysis.

The option of increasing the power of the generators up to 200 kW is studied in two ways, the capacity of the collection grid to dispatch this amount of power is enough and shows no problem, the economical aspect shows that layout 1 is still the best option among the three presented.

The compliance with the grid code of the UK is studied. Requirements regarding voltage fluctuation and power factor are accomplished by the proposed wave farm. Considering the worst case scenario the voltage fluctuations are below 3% and the limits is set to 10%. Frequency deviations are not an issue since the generators interface the grid through a fully-rated converter, the high-frequency harmonics resulting from the commutation of the converters can be filtered at the PCC to comply with the regulations. An assessment for dimensioning the DC-chopper that protects the converters and generators during grid faults is provided.

Wave energy presents a pulsating nature, as a consequence, flicker emissions may be a major concern, furthermore special attention is put on flicker analysis. The flicker coefficients of the wave farm using the gravity weight accumulator and considering the worst case regarding the amplitude (i.e. all units are generating the same amount of power simultaneously) are within the limits established by the grid code. The short term flicker emissions for this case are between 0.02 and 0.09 when and limit allowed (according to the IEC) is 0.2. The same analysis is performed but using the captured power (i.e. without using the gravity weight accumulator) showing that the limits are violated in this case going up to 0.67 in the worst case.

Since generally not all the units are acting simultaneously the IEC establishes a factor (the square root of the number of units) to consider the smoothing effect that several non-coordinated generators produce in the power delivered. By using this factor the flicker coefficients of the captured power of the wave farm fall again within the limits of the regulations, however it is important to remark that this factor may be too optimistic and a 20% increase in these value has been reported in the case of wind farms.

A realistic situation is proposed where the wave farm is connected to the Degerham switchgear station which is where currently the Utgrunden wind farm is connected. The flicker emissions increase in this case but still comply with the regulations, since wave farms (and also wind farms) are usually located

in remote areas it is expected to be connected to weak grids which are more influenced by voltage fluctuations and flicker effects.

The use of aggregated models show, as expected, a reduction of the flicker emission with respect to the single model used previously. This reduction is down to around 1/3 in the case of the group model and 1/9 for the park model, i.e. the flicker coefficients of the group model are a third of the flicker coefficients obtained using the single model and a ninth when the comparison is made between the park model and the single model. Similar results are obtained in the case of the non-smoothed power. According to this results, if the group model is selected, the amount of energy storage capacity can be reduced so that the power fluctuation increases a 250% without risk of exceeding the flicker emissions limit in the Utgrunden example. It has been also shown the dependency of the flicker emissions on the grid connection point although the flicker coefficients can provide an indication of the flicker level of the wave park under study. It is worth to highlight that wave parks and wind farms are usually located in remote areas and connected to weak grids and therefore flicker emissions should be reduced as much as possible in order to comply with the local grid code.

In a final analysis the life-cycle of the installation show that a share of approximately 30€ of the electricity price will be required to cover the expenses of the electrical system of the wave farm. This result provides a hint of how much that can be invested in the wave farm units to have an economically viable project. The costs share of the different aspects involved in the electrical system of the wave farm are provided in this analysis as well.

Bibliography

[1] XLPE Cable Systems, User's guide. ABB Revision 2. 13

[2] ElByggnadsRationalisering Kostnadskatalog 2012. (www.svenskenergi.se) 14

[3] National Grid Electricity Transmission, UK, The grid code. Issue 5. Revision 2. January 2013. 28, 30

[4] Marian P. Kazmierkowski and Marek Jasinski. Power Electronics for Renewable Sea Wave Energy. In Proceedings of 12th International Conference on Optimization of Electrical and Electronic Equipment, OPTIM 2010. 6

[5] Tarek Ahmed, Katsumi Nishida and Mutsuo Nakaoka. The Commercial Advancement of 16 MW Offshore Wave Power Generation Technologies in the Southwest of the UK. In Proceedings of 8th International Conference on Power Electronics, ECCE Asia. June 2011. 6

[6] U.S. Department of the Interior, Minerals Management Service. Proserv Offshore. Decommissioning Cost Update for Removing Pacific OCS Region Offshore Oil and Gas Facilities. Project No. 29056-11. January 2010. 40

[7] A report prepared by the RAMBOLL and LNEG to the OES-IA under the Annex II - Guidelines for Development and Testing of Ocean Energy Systems. Task 1.1 Generic and Site-related Wave Energy Data. September 2010. OES-IA Document n^o T02-1.1 5

[8] Stefan Lundberg. Performance comparison of wind park configurations. Technical report 30R. Department of Electric Power Engineering. Chalmers University of Technology. Sweden 2003. 14